Contents list available at CBIORE journal website

International Journal of Renewable Energy Development

Journal homepage: https://ijred.cbiore.id

Research Article

Immobilized L-arginine on methacrylate polymer as reusable heterogeneous catalyst for crude palm oil transesterification

Erwanto Erwanto[a,b*], Warsito Warsito[a], Akhmad Sabarudin[a], Diah Mardiana[a], Elvina Dhiaul Iftitah[a*]

[a]*Department of Chemistry, Faculty of Mathematics and Natural Sciences, Universitas Brawijaya, 65145 Malang City, Indonesia*

[b]*Department of Chemistry, Faculty of Science and Technology, Universitas Bojonegoro, 62119 Bojonegoro, Indonesia*

Abstract. The development of enviromentally friendly and reusable heterogenous catalyst has attracted significant attention for sustainable biodiesel production from low-cost feedstocks such as crude palm oil (CPO). This study aims to synthesize and evaluate an L-arginine immobilized methacrylate-based porous polymer as an efficient and reusable heterogenous base catalyst for CPO transesterification. In this study, a porous polymer synthesized from glycidyl methacrylate (GM) and ethylene glycol dimethacrylate (EGD), denoted as poly(GM-co-EGD), was employed as a support matrix for L-arginine immobilization to develop an efficient heterogeneous base catalyst for the transesterification of CPO. The catalyst was prepared via free radical polymerization followed by covalent immobilization of L-arginine onto the porous polymer framework. FESEM analysis revealed a well-developed interconnected porous morphology, which was further supported by textural characterization showing a high BET surface area of 650 $m^2\ g^{-1}$ and a total pore volume of 2.07 $cm^3\ g^{-1}$. FTIR spectra confirmed the successful chemical bonding between L-arginine and the polymer matrix. Thermogravimetric analysis indicated good thermal stability of the polymeric catalyst up to 120 °C, suitable for transesterification conditions. The basic strength evaluated using Hammett indicators showed moderate-to-strong basicity ($9.9 < H_- < 12$), while quantitative back titration with benzoic acid revealed that the catalyst with a poly(GM-co-EGD):L-arginine ratio of 1:2 exhibited the highest total basicity of 1.01 mmol g^{-1}. Process optimization using Response Surface Methodology with a Box–Behnken design produced a highly accurate quadratic model ($R^2 = 0.9992$). Under optimal conditions, a biodiesel yield of 82.34 ± 1.08% was achieved, consistent with model predictions. The catalyst maintained stable performance over five consecutive cycles, demonstrating its potential as a green and sustainable catalyst for biodiesel production from CPO.

Keywords: L-Arginine; Immobilization; Polymer; Box Behnken Design; transesterification.

Received: 13th Sept 2025; Revised: 18thJanuary 2026; Accepted: 16th Feb 2026; Available online: 1st March 2026

1. Introduction

Recent studies have focused on base catalysts that promote the reaction of triglycerides with methanol, aiming to increase biodiesel yield and support sustainable production (Ali Ijaz Malik *et al.,* 2024; Mahmudul *et al.,* 2017). The growing trend in basic catalyst development demonstrates significant potential in improving catalytic performance, particularly in biodiesel synthesis (Yusuf *et al.,* 2024). Homogeneous catalysts like KOH, NaOH, and CH_3ONa are widely used due to their ability to accelerate the transesterification process efficiently and economically, often resulting in high biodiesel yields (Lin & Tseng, 2024; Riaz *et al.,* 2024). However, challenges arise in the recovery and separation of homogeneous catalysts, which can generate alkaline salt waste (Abed *et al.,* 2025). Moreover, the purification steps required after reaction with homogeneous alkali catalysts are technically complex and economically burdensome (Wan Osman *et al.,* 2024). As a result, the development of efficient, recoverable, and environmentally friendly catalysts has become a priority, in line with the increasing attention to green chemistry principles and economic sustainability.

Heterogeneous catalysts present a promising alternative because they can be reused and easily removed after the reaction, thereby avoiding the complex purification steps required in homogeneous systems (Ponnumsamy *et al.,* 2024; Salaheldeen *et al.,* 2021). Several highly reactive heterogeneous base catalysts have been reported, including CaO (Davoodbasha *et al.,* 2021; Hadiyanto *et al* 2016), NiO (Ahmad *et al.,* 2023; Satriadi *et al* 2022) and K_2FeO_4 (Mena-cervantes et *al.,* 2022), which are classified as metal oxides. However, these single-metal catalysts often suffer from leaching during the reaction, which transforms the system into a semi-homogeneous one and thus diminishes the primary advantage of heterogeneity (Prats et *al.,* 2020; Vasić, 2020; Zhao *et al.,* 2019)

An alternative approach involves the use of lipase enzymes as biocatalysts, which offer several advantages, including higher energy efficiency, milder reaction conditions, and better tolerance to free fatty acids (FFAs) and water (Farobie *et al.,* 2021; Muanruksa *et al.,* 2021). However, challenges such as variability in enzyme activity and susceptibility to deactivation remain significant limitations. To address these issues, enzyme immobilization on solid supports has been extensively explored to improve stability and reusability. Despite these

* Corresponding author
Email: erwantokimia@gmail.com (Erwanto); vin_iftitah@ub.ac.id (E. D. Iftitah)

https://doi.org/10.61435/ijred.2026.61761
ISSN: 2252-4940/© 2026.The Author(s). Published by CBIORE

advancements, immobilized enzyme systems often face diffusion limitations and mass transfer constraints, which can hinder overall reaction rates (Alotaibi *et al.,* 2018; Carvalho et *al.,* 2018; Giraldo *et al.,* 2023; Gusniah *et al.,* 2020; Lv *et al.,* 2014; Urban *et al.,* 2012; Xie & Huang, 2020).

Recent studies have highlighted the role of L-arginine as an effective active site for transesterification in biodiesel production (Cavalcante *et al.,* 2021). In particular, its combination with ionic liquids as cationic counterparts has been shown to facilitate the transesterification of vegetable oils, including sunflower oil (Li & Guo, 2017b, 2017a). In contrast, unmodified L-arginine shows little to no catalytic activity, primarily due to the lack of cationic functional groups. Interestingly, crude palm oil (CPO), which naturally contains phospholipids and sterols (Mba *et al.,* 2015) may serve as an intrinsic source of cationic species, potentially enhancing the catalytic performance of L-arginine without the need for additional modification.

To improve its stability and reusability, L-arginine must be functionalized into a heterogeneous catalyst through immobilization onto a polymer-based support. Methacrylate-based polymers, which contain epoxy groups, provide reactive functional sites that enable covalent bonding with L-arginine. Previous studies have reported that these epoxy groups are also effective in binding enzymes with structural similarities to arginine, thereby reducing the risk of catalyst leaching during the reaction and improving operational stability. Furthermore, the addition of porogenic agents during the synthesis of porous polymers can enhance surface area and generate interconnected pore structures, which promote greater accessibility to the active catalytic sites (Amalia *et al.,* 2021; Sabarudin *et al.,* 2021; Xie & Huang, 2020; Widayat *et al* 2024).

In this work, L-arginine was immobilized onto poly(GM-co-EGD), with a focus on evaluating of covalent bonding efficiency between arginine and the polymer, the morphology and pore structure of the support, and the determination of catalytic strength and basicity. Furthermore, to optimize biodiesel production from CPO, catalytic performance was assessed using Response Surface Methodology with a Box–Behnken Design (RSM-BBD), allowing for a structured analysis of critical process parameters and determination of optimal conditions. In addition, the study examined the catalyst's reusability over multiple cycles to assess its long-term operational stability.

2. Materials and Methods

2.1 Materials

All reagents applied in this work were of analytical grade and utilized without additional purification. As porogenic solvents, 1,4-butanediol ($C_4H_{10}O_2$, ≥99%) and 1-propanol (C_3H_8O, ≥99.5%) were purchased from Merck (Germany). The polymerization initiator was 2,2′-azobisisobutyronitrile (AIBN, $C_8H_{12}N_4$, 12 wt.% in acetone, Merck, Germany). Crude palm oil (CPO), containing about 2% free fatty acids (FFA), was employed as the raw material for biodiesel synthesis. Ethanol (C_2H_5OH, ≥99.8%, Merck, Germany) was used during the washing and purification steps.

Glycidyl methacrylate (GM, $C_7H_{10}O_3$, ≥97.0%) as the functional monomer and the copolymer was synthesized using ethylene glycol dimethacrylate (EGD) as the crosslinking agent, both supplied by Merck (Germany). Monomer and crosslinking agent was used to enhance the rigidity of the polymer network. L-Arginine ($C_6H_{14}N_4O_2$, ≥98%, Merck, Germany) was immobilized onto the polymer as the active catalytic species.

Methanol (CH_3OH, ≥99.9%, Merck, Germany) was used as the alcohol reactant in the transesterification process. Pyridine (C_5H_5N, ACS reagent, ≥99.0%) served as a solvent and catalyst modifier. For neutralization and washing procedures, sodium bicarbonate ($NaHCO_3$, ≥99.0%), sodium carbonate (Na_2CO_3, ≥99.5%) and sodium hydroxide (NaOH, ≥99.0%) were used. Finally, anhydrous sodium sulfate (Na_2SO_4, ≥99%) was used to absorb any remaining moisture during sample preparation.

2.2 Synthesis of Poly(GM-co-EGD)

The supported polymer was synthesized by adapting a modified previous research method (Amalia *et al.,* 2021), glycidyl methacrylate (GM) was used as the monomer (%T 40) and ethylene glycol dimethacrylate (EGD) as the crosslinker (%C 25). In a glass vial, the components were combined with a porogen composed of 1,4-butanediol, 1-propanol, and distilled water in a 4:7:1 (v/v) ratio. Homogenization was carried out using sonication for 5 minutes. AIBN (1% w/v) was then introduced as the initiator, and the mixture was further sonicated for 5 minutes. The vial was tightly sealed and maintained in an oven at 60 °C for 12 hours to ensure full polymerization. Once polymerization was complete, the formed polymer was extracted from the vial and cleaned by stirring it in ethanol and distilled water for 30 minutes under magnetic agitation. The resulting polymer was designated as poly(GM-co-EGD), and the synthesis steps are illustrated in Figure 1.

2.3 Immobilization of L-arginine

The immobilization of L-arginine was carried out through a reaction between the epoxy groups on the methacrylate-based poly(GM-co-EGD) and the amine groups of L-arginine. In this process, poly(GM-co-EGD) was reacted with L-arginine under basic conditions to form secondary amine linkages. To prepare

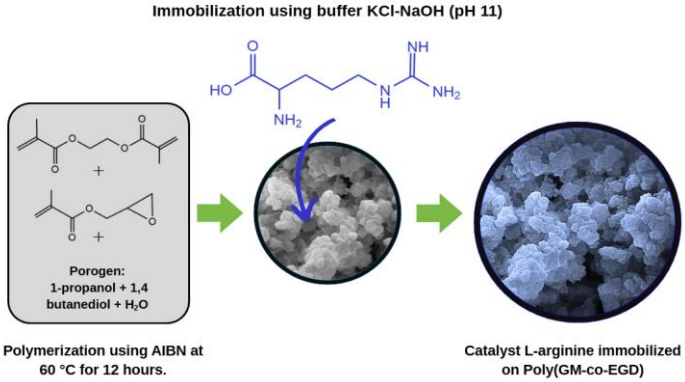

Fig 1. Schematic synthesis and immobilization procedure

Table 1
The range and coded value (independent variables) of Box–Behnken design.

Parameter	Symbol	Unit	Coded Value		
			Low (-1)	Center (0)	High (+1)
Reaction time	A	(minutes)	60	150	240
Catalyst Loading	B	(wt %)	1	3	5
Me-OH:Oil molar ratio	C	(-)	4	12	20

the L-arginine solution, 10 mg/mL of the compound was dissolved in a 0.2 M KCl–NaOH buffer with a pH of 11, and this solution was subsequently mixed with the polymer support to initiate the immobilization process. The reaction proceeded at 25 °C (298 K) for 120 minutes, with mass ratios of poly(GM-co-EGD) to L-arginine (1:1, 1:2, and 2:1) being tested in order to investigate how the ratio affects the immobilization efficiency, as illustrated in Figure 1. The resulting material was designated as L-arginine immobilized on poly(GM-co-EGD).

2.4 Characterization of Polymer Catalyst

Fourier Transform Infrared (FTIR) spectroscopy (IRSpirit-T/ATR, Shimadzu) was used to analyze the functional groups of the synthesized polymer and the L-arginine-immobilized polymer. The morphology of the polymer was observed using a Field Emission Scanning Electron Microscope (FESEM) (FEI Quanta 650 FEG). Thermal stability was evaluated using a Shimadzu DTG-60 thermogravimetric analyzer over a temperature range of 25–1100 °C. The instrument has a measurable range of ±500 mg (TG) with a weight resolution of 0.1 µg. All measurements were conducted under either air or an inert gas atmosphere. Surface area and pore characteristics were determined using a Quantachrome Novatouch LX4 surface area analyzer.

The basic strength of L-arginine, poly(GM-co-EGD), and the immobilized catalyst was determined using the Hammett indicator method with bromothymol blue (H^- = 7.2), phenolphthalein (H^- = 9.8), *p*-nitrotoluene (H^- = 12), and 2,4-dinitroaniline (H^- = 15.0). Approximately 250 mg of sample was added to each indicator solution in methanol, and the color change was observed to estimate the basic strength range. The total basicity was further quantified by titration with 0.01 N benzoic acid after dispersing the catalyst in benzene, with the endpoint determined by the disappearance of the indicator color. The catalyst exhibiting the highest basic strength and total basicity was subsequently selected for further optimization of reaction parameters. (Chueluecha *et al.,* 2017a; Malek *et al.,* 2021; Roschat *et al.,* 2016; Zhang *et al.,* 2023).

2.5 Experimental Design

The optimization of transesterification reaction parameters was carried out using the RSM-BBD framework, designed and analyzed with Design-Expert 13. Three factors were chosen as independent variables, each tested at three coded levels (low, medium, and high), as summarized in Table 1. These ranges and coded settings were supplied to the program to obtain the design matrix.

The design produced a total of 17 experimental runs, comprising 12 factorial and axial combinations and 5 center points used for model replication and validation. The number of runs was determined using the standard RSM-BBD formula: $k^2 + k + c_p$, where k is the number of independent variables (k = 3), and c_p is the number of center point replications. Each experiment was performed in triplicate to ensure consistency and statistical reliability. The average biodiesel yield from the replicates was used as the response variable. The complete

Table 2
Transesterification experimental matrix generated by BBD, with corresponding actual and predicted biodiesel yields.

Run	Variable			Biodiesel Yield (%)		Residual
	A	B	C	Predicted	Actual	
1	150	3	12	66.96	67.95	0.995
2	150	5	4	51.04	50.945	-0.0944
3	60	1	12	36.07	35.64	-0.4275
4	150	1	20	45.24	45.33	0.0944
5	240	3	4	52.22	51.89	-0.3331
6	240	5	12	80.7	81.13	0.4275
7	150	3	12	66.96	66.11	-0.845
8	150	5	20	69.79	69.63	-0.1644
9	60	3	4	34.95	35.215	0.2631
10	150	3	12	66.96	66.75	-0.205
11	240	3	20	73.78	73.52	-0.2631
12	60	5	12	48.66	48.49	-0.1688
13	150	1	4	37.23	37.39	0.1644
14	240	1	12	54.92	55.09	0.1687
15	150	3	12	66.96	67.05	0.095
16	150	3	12	66.96	66.915	-0.04
17	60	3	20	40.16	40.49	0.3331

experimental matrix, including both actual and predicted biodiesel yields, is shown in Table 2.

To capture the relationship between biodiesel yield and the independent variables, a second-order (quadratic) polynomial model was applied. The efficiency of biodiesel production was modeled as a function of the three independent variables using a second-order polynomial equation, as presented in Eq 1.

$$Y = \beta_0 + \sum_{i=1}^{3} \beta_i x_i + \sum_{i=1}^{3} \beta_{ii} X_i^2 + \sum_{i=1}^{2} \sum_{j=i+1}^{3} \beta_{ij} X_i X_j \quad (1)$$

where Y is the predicted response; β_0 is the intercept; β_i, β_{ii}, and β_{ij} represent the linear, quadratic, and interaction regression coefficients, respectively, corresponding to the effects of the independent variables, their curvature contributions, and their combined interactions.

2.6 Biodiesel Analysis

Optimal reaction conditions for the transesterification of CPO with immobilized L-arginine catalyst on poly(GM-co-EGD) were first determined. The resulting biodiesel was subsequently characterized for its composition by GC–MS, and the reported yields represent the average of two independent runs. Biodiesel yield was calculated using Equation (2):

$$\text{Biodiesel yield (\%)} = \frac{\text{Mass of biodiesel obtained}}{\text{Initial mass of CPO}} \times 100 \quad (2)$$

where the mass of biodiesel obtained refers to the purified fatty acid methyl esters (FAMEs) collected after reaction and separation.

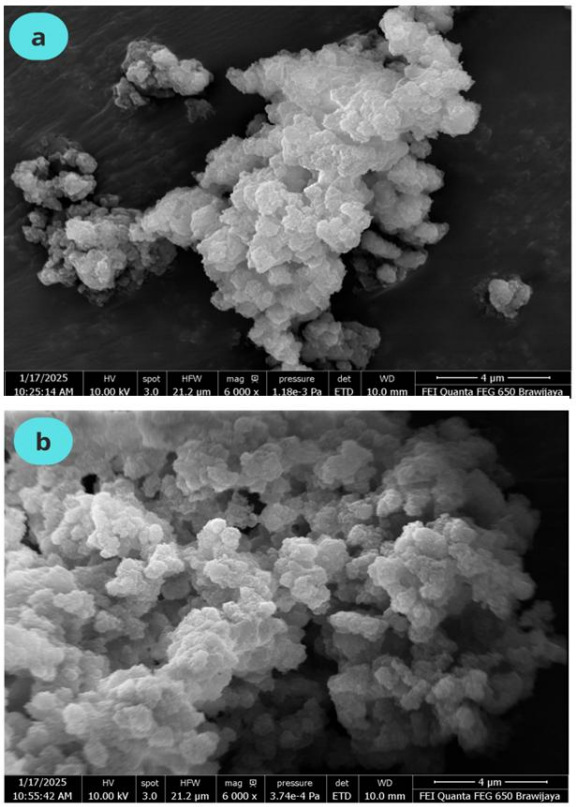

Fig 3. Surface morphology observed by SEM for (a) Poly(GM-co-EGD) and (b) L-Arginine immobilized poly(GM-co-EGD) at 6000x magnification each.

3. Results and Discussion

3.1 Characterization and Catalyst Verification

Evidence of successful immobilization of L-arginine on poly(GM-co-EGD) was obtained from FTIR-ATR and FESEM analyses. The FTIR spectrum (Figure 2) exhibited peaks at 910 cm^{-1} and 840 cm^{-1}, arising from the epoxy groups of glycidyl methacrylate (GM), thus confirming their presence within the polymer network. Following the immobilization of L-arginine, these epoxy bands showed a marked decrease in intensity, accompanied by the appearance of a broad absorption band in the 3300–3100 cm^{-1} region, corresponding to N–H stretching vibrations. These changes suggest that a nucleophilic reaction occurred between the amine groups of L-arginine and the epoxy rings, leading to covalent bond formation (Amalia *et al.,* 2021; Tasfiyati *et al.,* 2016).

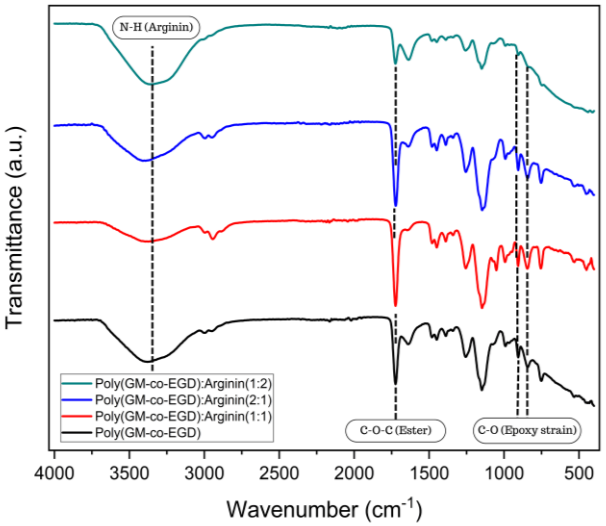

Fig 2. FTIR spectrum of Poly (GM-co-EGD), Poly (GM-co-EGD) immobilized Arginine (1:1; 1:2; 2:1)

Morphological observations using field-emission SEM (Figure 3) showed that poly(GM-co-EGD) possesses a three-dimensional porous surface. The incorporation of EGD as a cross-linking agent promoted the formation of an interconnected microglobular network, as observed in both the neat poly(GM-co-EGD) (Figure 3a) and the L-arginine-immobilized polymer (Figure 3b). The material exhibited a relatively homogeneous porous morphology without significant structural collapse after immobilization, indicating that the polymer framework remained intact.

These morphological findings are further supported by textural characterization results. The material exhibits a high BET surface area of 650 $m^2\ g^{-1}$ and a total pore volume of 2.07 $cm^3\ g^{-1}$, confirming the formation of a well-developed and interconnected porous polymeric structure. The combination of SEM and BET analyses validates the successful synthesis of a stable porous network, which is essential for enhancing active site accessibility and facilitating mass transfer in heterogeneous catalytic applications.

Based on the TGA results (Figure 4), the polymer exhibits four distinct stages of thermal degradation. An initial weight loss of 10.62% up to ~120 °C is attributed to the removal of adsorbed moisture and volatile species. This is followed by a 32.18% weight loss in the range of 120–200 °C, associated with the decomposition of thermally less stable functional groups. The main degradation occurs between 250 and 320 °C, with a

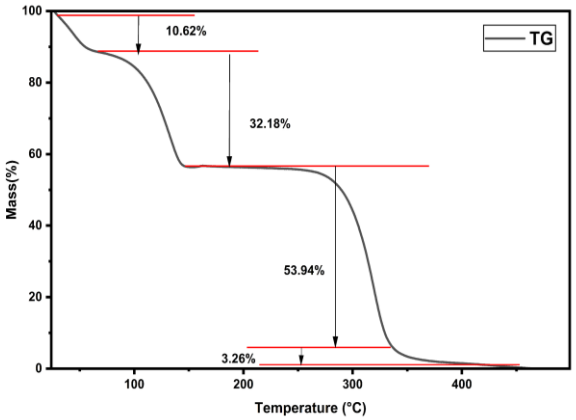

Fig 4. TGA Thermogram of Poly (GM-co-EGD)

Table 3
Basicity of L-Arginin and Poly(GM-co-EGD)@L-Arginin

Catalyst	Basic amount mmol g^{-1}
L-Arginin	1.54
poly (GM-co-EGD)@L-Arginin (1:1)	0.62
poly (GM-co-EGD)@L-Arginin (2:1)	0.76
poly (GM-co-EGD)@L-Arginin (1:2)	1.07

significant mass loss of 53.94% corresponding to polymer backbone scission. Above 350 °C, only 3.26% residue remains, indicating the predominantly organic nature of the material. Importantly, the polymer demonstrates good thermal stability up to approximately 120 °C, which is well above the typical temperature range employed in transesterification reactions. This confirms that the catalyst structure remains intact under reaction conditions, minimizing thermal deactivation during biodiesel synthesis. Compared with poly(GM-co-EGD) reported by (Chitanda *et al.,* 2015), the present material shows a more complex degradation profile and improved thermal stability, which can be attributed to differences in the porogen system used during polymer synthesis.

The basic strength of poly(GM-co-EGD), free L-arginine, and immobilized L-arginine catalysts was qualitatively evaluated using Hammett indicators (bromothymol blue, phenolphthalein, p-nitrotoluene, and 2,4-dinitroaniline). Color changes were observed for all indicators except 2,4-dinitroaniline, indicating that the catalyst possesses basic sites within the range of $7.2 < H_- < 12$. This confirms the presence of medium to strong basic sites attributed to the guanidine functionality of immobilized L-arginine. To quantitatively determine the total basicity, back titration using 0.01 N benzoic acid was performed (Table 3). The results show that the catalyst prepared with a poly(GM-co-EGD) to L-arginine ratio of 1:2 exhibited the highest basicity, reaching 1.01 mmol g^{-1}. This indicates that increasing the L-arginine loading enhances the density of accessible basic sites, up to the optimal immobilization ratio.

3.2 RSM-BB Design (Response Surface Methodology via Box–Behnken Design)

3.2.1 Quadratic Polynomial Model Formulation

A total of 17 transesterification experiments were designed to explore the effects of 3 key variables: reaction time (A), catalyst loading (B), and Me-OH:Oil molar ratio (C), as outlined in Table 2. To assess how each factor—and their interactions—influenced biodiesel yield, a second-order (quadratic) polynomial model was employed. Equation (3) presents the regression model obtained from the analysis, describing the relationship between the variables and biodiesel yield):

$$Y\,\% = 66.96 + 12.72\,A + 9.59\,B + 6.69\,C + 3.30\,AB + 4.09\,AC + 2.69\,BC - 6.21\,A^2 - 5.66\,B^2 - 10.47\,C^2 \quad (3).$$

In this model, Y denotes the predicted biodiesel yield (%), while AB, AC, and BC represent the interaction effects between pairs of variables. A^2, B^2, and C^2 indicate the nonlinear (quadratic) influence of reaction time, catalyst loading, and Me-OH:Oil molar ratio, respectively, on biodiesel yield. Positive coefficients suggest that increasing the respective variable enhances biodiesel yield, while negative coefficients reflect a diminishing effect.

As shown in the perturbation plot (Figure 5a), the individual effects of A, B, and C on biodiesel yield are depicted by measuring their deviation from the reference point in coded units. The slope of each curve indicates the sensitivity of biodiesel yield to changes in the respective variable, assuming other variables are held constant. Among the three, A exhibits the steepest curve, suggesting it has the most significant effect on biodiesel production, followed by C and B in the order A > C > B. This finding is consistent with the ANOVA results (Table 4), which show that reaction time has the highest F-value (3472.02), followed by C (1973.47) and B (960.12), confirming it as the dominant factor influencing the transesterification process.

Figure 5b provides additional validation of the model's accuracy, with experimental results closely matching the regression predictions. The concentration of points near the 45° line indicates minimal deviation between observed and predicted biodiesel yields. Such consistency demonstrates that the developed model effectively reflects variations in process conditions and is dependable across the experimental scope.

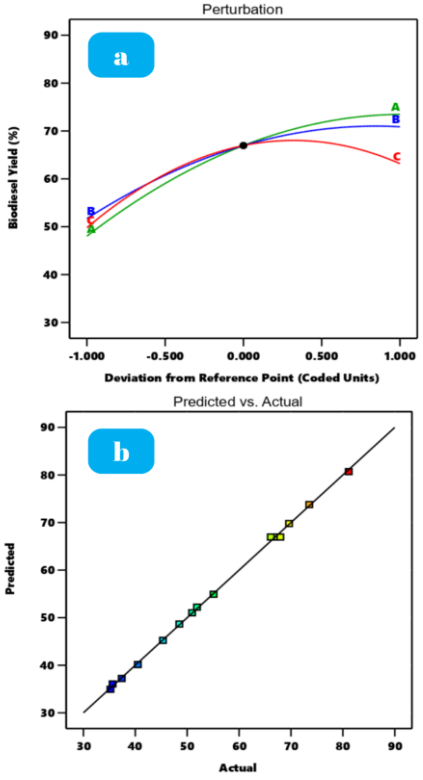

Fig 5. (a) Perturbation plot (b) Actual vs. predicted plot

Table 4
ANOVA Summary for the Quadratic Model of Biodiesel Yield (%)

Source	Sum of Squares	df	Mean Square	F-value	p-value	
Model	3367.07	9	374.12	1002.83	< 0.0001	significant
A-Reaction Time	1295.28	1	1295.28	3472.02	< 0.0001	
B-Catalyst Loading	736.22	1	736.22	1973.47	< 0.0001	
C-Methanol to Oil	358.18	1	358.18	960.12	< 0.0001	
AB	43.49	1	43.49	116.59	< 0.0001	
AC	66.87	1	66.87	179.25	< 0.0001	
BC	28.86	1	28.86	77.37	< 0.0001	
A^2	162.18	1	162.18	434.72	< 0.0001	
B^2	134.95	1	134.95	361.73	< 0.0001	
C^2	461.56	1	461.56	1237.23	< 0.0001	
Residual	2.61	7	0.3731			
Pure Error	1.76	3	0.2849	0.6487	0.6238	not significant
Lack of Fit	0.8547	4	0.4392			
Cor Total	3369.68	16				

Table 5
Model effectiveness parameters

Statistics	Value
R^2	0.9992
Adeq Precision	97.6633
Adjusted R^2	0.9982
Std. Dev.	0.6108
Predicted R^2	0.9951
C.V. %	1.08
Mean	56.44

3.2.2 ANOVA and Model Validation

The ANOVA results (Tables 4 and 5) confirm that the developed quadratic polynomial model is highly significant for predicting biodiesel yield (model $p < 0.0001$), with a non-significant lack-of-fit ($p = 0.6238$), indicating good model adequacy. The high coefficient of determination ($R^2 = 0.9992$), together with the close agreement between adjusted R^2 (0.9982) and predicted R^2 (0.9951), demonstrates excellent predictive capability. The adequate precision value (97.66) and low coefficient of variation (CV = 1.08%) further indicate a strong signal-to-noise ratio and high experimental reproducibility.

All interaction terms (AB, AC, and BC) were statistically significant ($p < 0.0001$), confirming that biodiesel yield is governed by coupled variable effects rather than independent contributions. Among them, the reaction time–methanol-to-oil ratio interaction (AC) showed the strongest influence, highlighting the interplay between kinetic progression and equilibrium shift. Increasing methanol promotes ester formation, but sufficient reaction time is required to realize this effect.

The reaction time–catalyst loading interaction (AB) also contributed substantially, indicating that the benefit of higher catalyst concentration depends on reaction duration, with diminishing incremental impact as equilibrium is approached. Although the catalyst loading–methanol ratio interaction (BC) exhibited the smallest effect among the interaction terms, it remained significant, reflecting the balance between active site availability and phase behavior, particularly in relation to glycerol solubility and reactant–catalyst contact.

3.2.3 Contour and Response Surface Analysis

The two-dimensional contour and three-dimensional surface plots in Figures 6a–c illustrate the interactions between process variables affecting the transesterification reaction, highlighting how changes in these parameters influence the outcome. Several contour plots exhibit elliptical shapes, suggesting significant interactions between the investigated variables. Conversely, circular contours imply weak or insignificant interactions. Complex and non-linear contour shapes further indicate that the relationships among variables are not straightforward. Each graph illustrates how two independent variables interact while keeping the third variable fixed at its midpoint. The graphical results reveal that the interaction of these effects significantly governs the overall reaction performance. This confirms that the RSM-BBD approach is a powerful tool for pinpointing the optimal conditions to maximize biodiesel production.

In Figure 6a, increasing both catalyst loading and reaction time positively influence biodiesel production efficiency. A rise in catalyst loading from 1% to 5% (w/w) led to a notable improvement in biodiesel yield, although further increases beyond this point showed no additional advantage. This phenomenon may be attributed to mixing limitations and increased solution viscosity due to excess catalyst, which could hinder optimal mass transfer. These results are in agreement with earlier research indicating that excessive catalyst loading can negatively impact the overall performance of the transesterification reaction (Mohadesi *et al.,* 2021).

Figure 6b shows that the interaction between Me-OH:Oil molar ratio and reaction time plays a critical role in enhancing biodiesel yield. Increasing the Me-OH:Oil molar ratio from 1:4 to 1:12, along with extending the reaction time from 60 to 240 minutes, led to a steady improvement in production efficiency. A higher methanol ratio facilitates better solubilization of triglycerides (TG), leading to more effective contact between reactant molecules (Parandi *et al.,* 2023). Moreover, prolonged reaction time provides sufficient opportunity for the reaction to reach completion. However, once the methanol ratio exceeds the optimum point, the improvement in efficiency levels off or even declines, likely due to the dilution effect on both reactants

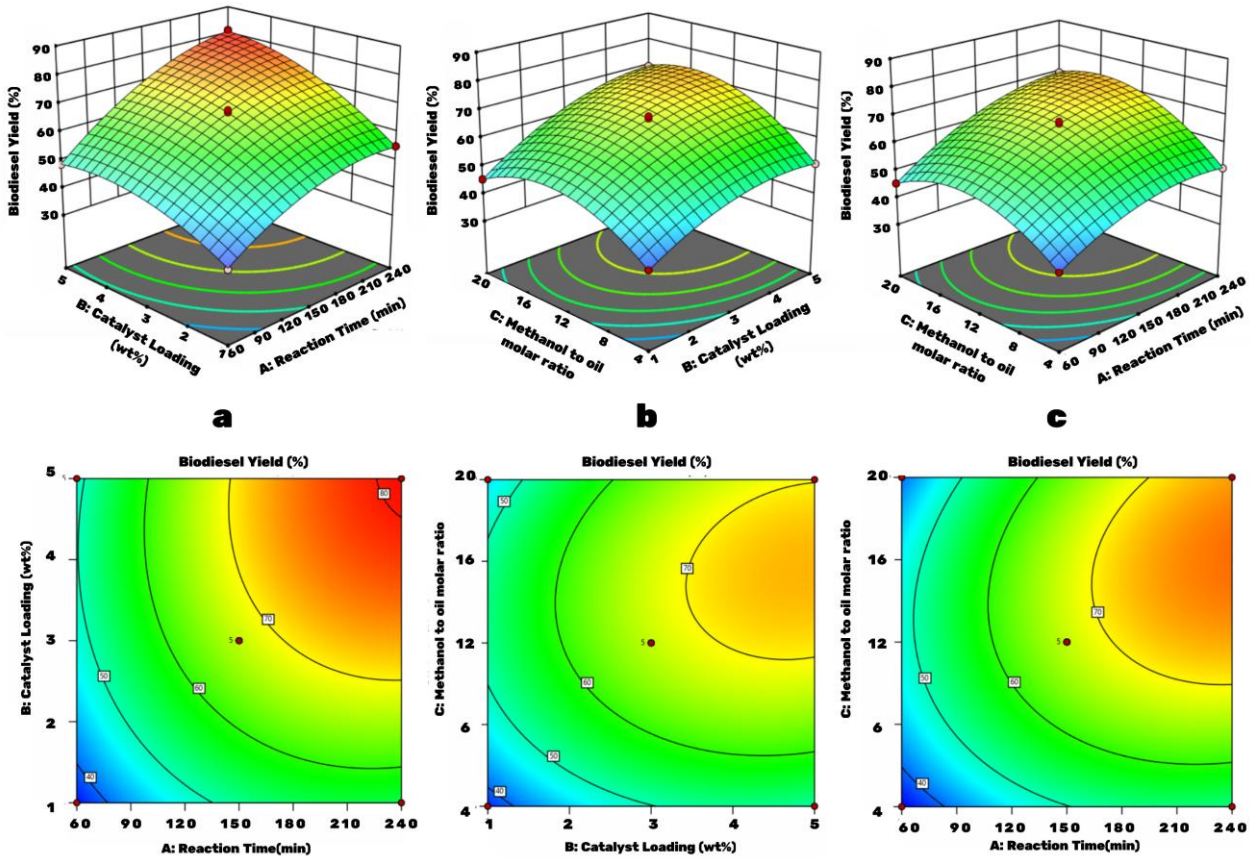

Fig 6. 3D response surface and 2D contour plots showing the effects of: (a) reaction time(min) and catalyst loading (wt%), (b) Molar ratio of Me-OH:Oil and reaction time (min), and (c) Molar ratio of Me-OH:Oil and catalyst loading (wt%), on FAME efficiency.

and catalyst, which ultimately reduces reaction effectiveness. This result aligns with previous studies (Chueluecha *et al.*, 2017b).

Figure 6c also suggests that increasing both catalyst loading and Me-OH:Oil molar ratio contributes to improved biodiesel production, particularly when these variables remain within their optimal ranges. However, exceeding these optimal levels leads to a decline in efficiency. This may be because excessive methanol raises glycerol's solubility in the biodiesel, making it harder to separate and possibly causing catalyst deactivation. On the other hand, too much catalyst loading, exemplified by immobilized L-arginine on poly(GM-co-EGD), can thicken the reaction mixture. This condition restricts the movement of reactants, slowing down the reaction and lowering biodiesel output, a pattern also reported in prior research *(*Mohadesi *et al.,* 2021). The quadratic regression model was employed to identify the most favorable values of the variables within the tested range, with the objective of enhancing biodiesel production efficiency using L-arginine immobilized on poly(GM-co-EGD). As shown in Figure 7, the predicted maximum efficiency (83.08%) was achieved under the optimal conditions of reaction time (233.76 minutes), Me-OH:Oil molar ratio (14.595), and catalyst loading (4.67 wt%). To validate the proposed quadratic model, the transesterification process was

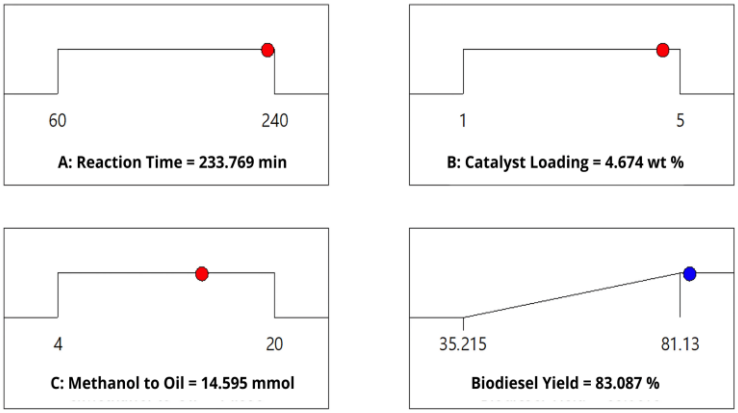

Fig 7. Optimization of effective variables in the transesterification process

Table 6.
The profile of FAMEs presence after transesterification reaction

Compound name	Content (wt%)	
	This Work	Dos Santos *et al.*, (2019)
Lauric acid	0.596	0.21
Myristic acid	2.434	0.72
Palmitic acid	52.729	40.59
Stearic acid	5.547	4.45
Arachidic acid	0.318	0.32
Palmitoleic acid	0.187	0.11
Oleic acid	28.131	43.26
Linoleic acid	9.562	9.72
Linolenic acid	0.314	0.23

conducted in triplicate under the identified optimal conditions. An average FAMEs yield of 82.34 ± 1.08% was obtained, demonstrating a close agreement between the experimental results and the model's predictions with no statistically significant difference. This confirms the strong consistency between predicted and actual biodiesel efficiencies.

For comparison, the use of free L-arginine under the same optimal parameters resulted in a higher biodiesel yield of 86.25%. This can be attributed to the direct availability of all basic functional groups without internal diffusion limitations or pore accessibility constraints that may occur in the immobilized system. Moreover, at an equivalent catalyst loading, free L-arginine exhibits higher intrinsic activity because all basic sites are directly exposed in the homogeneous reaction phase.

However, it should be noted that the reaction system did not specifically monitor or quantify the occurrence of saponification during the transesterification process. Therefore, although no visible soap formation or significant emulsion issues were observed during product separation, the possibility of minor saponification side reactions cannot be completely excluded. Further analysis, such as measuring soap content or performing saponification value determination, would be necessary to comprehensively evaluate the extent of side reactions under these conditions.

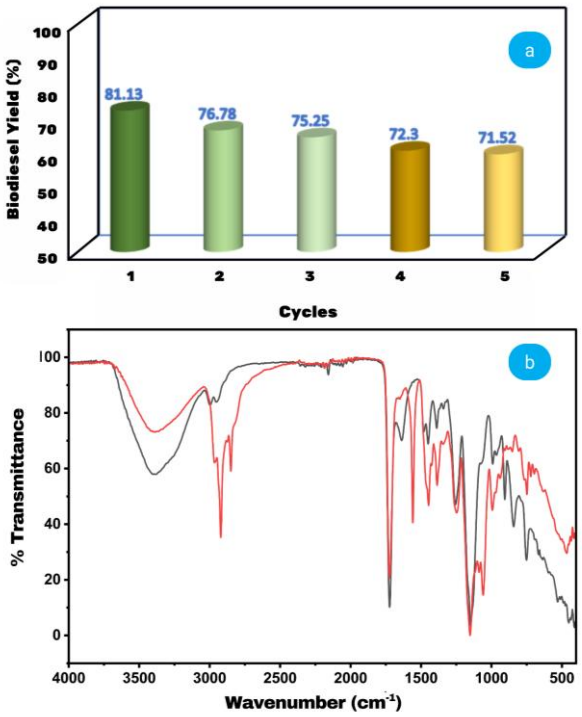

Fig 8. Reusability cycles (a) and FTIR spectra before and after use (b)

3.3 Biodiesel Specifications

GC-MS results demonstrated that triglycerides were effectively converted into FAMEs using the L-arginine immobilized poly(GM-co-EGD) catalyst, as shown in Table 6. When compared to previously reported biodiesel derived from CPO (dos Santos *et al.*, 2019), the FAME profile observed in this study shows a high degree of similarity, with methyl palmitate and methyl oleate emerging as the dominant components. Notably, the methyl palmitate content in the current biodiesel sample was higher than that reported in earlier studies, suggesting a more efficient conversion of saturated triglycerides. These findings indicate that the use of L-arginine as an immobilized catalyst enhances both the selectivity and efficiency of the transesterification process.

3.4 Stability and Reusability

The stability and reusability of L-arginine immobilized on poly(GM-co-EGD) were evaluated through five consecutive transesterification cycles. The catalytic activity for each cycle is presented in Figure 8a. After each reaction, the catalyst was separated by filtration and washed with methanol before being reused. The catalyst maintained relatively stable activity up to the fifth cycle, with only a slight decrease in performance.

The FTIR spectra before and after reuse are shown in Figure 8b. The spectrum of the catalyst after five cycles (red line) is consistent with that of the fresh catalyst (black line), with no noticeable shift or disappearance of the main characteristic bands. The broad band at approximately 3300–3400 cm^{-1} corresponds to –OH/–NH stretching vibrations, while the peaks at 2920–2850 cm^{-1} are attributed to aliphatic C–H stretching. The ester carbonyl (C=O) band appears at around 1720 cm^{-1}, and the C–N and C–O stretching vibrations are observed in the range of 1200–1050 cm^{-1}. The preservation of these bands confirms that the chemical structure of the catalyst remained stable during the reaction and regeneration processes, indicating that the slight decrease in activity was not caused by structural degradation.

4. Conclusion

This study demonstrates that L-arginine immobilized on porous poly(GM-co-EGD) exhibits suitable structural, chemical, and catalytic properties for transesterification applications. FESEM and textural analyses confirmed a well-developed three-dimensional porous structure with a high BET surface area of 650 $m^2\ g^{-1}$ and a total pore volume of 2.07 $cm^3\ g^{-1}$, enabling effective accessibility of active sites. FTIR analysis

verified the successful covalent bonding of L-arginine onto the polymer matrix. Quantitative basicity evaluation by back titration revealed that the catalyst prepared at a poly(GM-co-EGD):L-arginine ratio of 1:2 achieved the highest basicity of 1.01 mmol g^{-1}, which is favorable for biodiesel synthesis. Process optimization using the RSM–BBD approach resulted in a high biodiesel yield of 81.13% with excellent model accuracy (R^2 = 0.9992). The catalyst also demonstrated good stability over five consecutive cycles, highlighting the advantages of immobilized L-arginine over homogeneous systems. Overall, poly(GM-co-EGD)–supported L-arginine represents a promising green, stable, and reusable heterogeneous catalyst for sustainable biodiesel production from crude palm oil.

Acknowledgments

The authors gratefully acknowledge Universitas Brawijaya for providing laboratory facilities, particularly the Analysis and Measurement Laboratory and the Integrated Research Laboratory (LRT), Faculty of Science, for instrumental and analytical support. The authors also thank the Chemistry Laboratory, Universitas Bojonegoro, for additional laboratory support during this research.

Author Contributions: Erwanto Erwanto: Writing – original draft, Methodology, Investigation, Formal analysis. Akhmad Sabarudin: Writing – review & editing, Conceptualization, Formal analysis, and Validation. Warsito Warsito: Writing – review & editing, Supervision, Project administration. Elvina Dhiaul Iftitah: Writing – review & editing, Funding acquisition and Visualization.

Funding: This research was funded by the Flagship Basic Research (Penelitian Dasar Unggulan – PDU) Program, Fiscal Year 2025, under Contract No. 01046.17/UN/10.A0501/B/KS/2025.

Conflicts of Interest: The authors declare no conflict of interest.

References

Abed, K. M., Hayyan, A., Hizaddin, H. F., Hashim, M. A., Basirun, W. J., Saleh, J., & Hashim, N. A. (2025). Superiority of liquid membrane-based purification techniques in biodiesel downstream processing. *Renewable and Sustainable Energy Reviews*, *207*(September 2024), 114911. https://doi.org/10.1016/j.rser.2024.114911

Ahmad, M., Qureshi, N., Zafar, M., & Aman, S. (2023). Renewable energy production from novel and non-edible seed oil of Cordia dichotoma using nickel oxide nano catalyst *Fuel*, *332*(P1), 126123. https://doi.org/10.1016/j.fuel.2022.126123

Ali Ijaz Malik, M., Zeeshan, S., Khubaib, M., Ikram, A., Hussain, F., Yassin, H., & Qazi, A. (2024). A review of major trends, opportunities, and technical challenges in biodiesel production from waste sources. *Energy Conversion and Management: X*, *23*(May), 100675. https://doi.org/10.1016/j.ecmx.2024.100675

Alotaibi, M., Manayil, J. C., Greenway, G. M., Haswell, S. J., Kelly, S. M., Lee, A. F., Wilson, K., & Kyriakou, G. (2018). Lipase immobilised on silica monoliths as continuous-flow microreactors for triglyceride transesterification. *Reaction Chemistry and Engineering*, *3*(1), 68–74. https://doi.org/10.1039/c7re00162b

Amalia, S., Angga, S. C., Iftitah, E. D., Septiana, D., Anggraeny, B. O. D., Warsito, Hasanah, A. N., & Sabarudin, A. (2021). Immobilization of trypsin onto porous methacrylate-based monolith for flow-through protein digestion and its potential application to chiral separation using liquid chromatography. *Heliyon*, *7*(8), e07707. https://doi.org/10.1016/j.heliyon.2021.e07707

Carvalho, N. B., Vidal, B. T., Barbosa, A. S., Pereira, M. M., Mattedi, S., Freitas, L. D. S., Lima, Á. S., & Soares, C. M. F. (2018). Lipase immobilization on silica xerogel treated with protic ionic liquid and its application in biodiesel production from different oils. *International Journal of Molecular Sciences*, *19*(7). https://doi.org/10.3390/ijms19071829

Cavalcante, F. T. T., Neto, F. S., Rafael de Aguiar Falcão, I., Erick da Silva Souza, J., de Moura Junior, L. S., da Silva Sousa, P., Rocha, T. G., de Sousa, I. G., de Lima Gomes, P. H., de Souza, M. C. M., & dos Santos, J. C. S. (2021). Opportunities for improving biodiesel production via lipase catalysis. *Fuel*, *288*(July). https://doi.org/10.1016/j.fuel.2020.119577

Chitanda, J. M., Misra, P., Abedi, A., Dalai, A. K., & Adjaye, J. D. (2015). Synthesis and Characterization of Functionalized Poly (glycidyl methacrylate) -Based Particles for the Selective Removal of Nitrogen Compounds from Light Gas Oil : E ff ect of Linker Length. *Energy Fuels*, 29(3), 1881–1891 https://doi.org/10.1021/ef502210z

Chueluecha, N., Kaewchada, A., & Jaree, A. (2017a). Biodiesel synthesis using heterogeneous catalyst in a packed-microchannel. *Energy Conversion and Management*, *141*, 145–154. https://doi.org/10.1016/j.enconman.2016.07.020

Chueluecha, N., Kaewchada, A., & Jaree, A. (2017b). Enhancement of biodiesel synthesis using co-solvent in a packed-microchannel. *Journal of Industrial and Engineering Chemistry*, *51*, 162–171. https://doi.org/10.1016/j.jiec.2017.02.028

Davoodbasha, M. A., Pugazhendhi, A., Kim, J. W., Lee, S. Y., & Nooruddin, T. (2021). Biodiesel production through transesterification of Chlorella vulgaris: Synthesis and characterization of CaO nanocatalyst. *Fuel*, *300*(May), 121018. https://doi.org/10.1016/j.fuel.2021.121018

dos Santos, L. K., Hatanaka, R. R., de Oliveira, J. E., & Flumignan, D. L. (2019). Production of biodiesel from crude palm oil by a sequential hydrolysis/esterification process using subcritical water. *Renewable Energy*, *130*, 633–640. https://doi.org/10.1016/j.renene.2018.06.102

Farobie, O., Jannah, Q. R., & Hartulistiyoso, E. (2021). Biodiesel Production from Crude Palm Oil under Different Free Fatty Acid Content using Eversa® Transform 2.0 Enzyme. *International Journal of Renewable Energy Research*, *11*(4), 1590–1596. https://doi.org/10.20508/IJRER.V11I4.12338.G8366

Giraldo, L., Gómez-Granados, F., & Moreno-Piraján, J. C. (2023). Biodiesel Production Using Palm Oil with a MOF-Lipase B Biocatalyst from Candida Antarctica: A Kinetic and Thermodynamic Study. *International Journal of Molecular Sciences*, *24*(13). https://doi.org/10.3390/ijms241310741

Gusniah, A., Veny, H., & Hamzah, F. (2020). Activity and stability of immobilized lipase for utilization in transesterification of waste cooking oil. *Bulletin of Chemical Reaction Engineering and Catalysis*, *15*(1), 242–252. https://doi.org/10.9767/bcrec.15.1.6648.242-252

Hadiyanto, H., Lestari, S. P., & Widayat, W. (2016). Preparation and Characterization of Anadara Granosa Shells and CaCO3 as Heterogeneous Catalyst for Biodiesel Production. *Bulletin of Chemical Reaction Engineering & Catalysis*, *11*(1), 21-26. https://doi.org/10.9767/bcrec.11.1.402.21-26

Li, J., & Guo, Z. (2017a). Catalytic Biodiesel Production Mediated by Amino Acid- Based Protic Salts. *ChemSusChem*, *10*, 1792–1802. https://doi.org/10.1002/cssc.201700026

Li, J., & Guo, Z. (2017b). Structure Evolution of Synthetic Amino Acids-Derived Basic Ionic Liquids for Catalytic Production of Biodiesel. *ACS Sustainable Chemistry and Engineering*, *5*(1), 1237–1247. https://doi.org/10.1021/acssuschemeng.6b02732

Lin, C. Y., & Tseng, S. L. (2024). Investigation into the Fuel Characteristics of Biodiesel Synthesized through the Transesterification of Palm Oil Using a TiO2/CH3ONa Nanocatalyst. *Catalysts*, *14*(9). https://doi.org/10.3390/catal14090623

Lv, Y., Lin, Z., Tan, T., & Svec, F. (2014). *Preparation of Reusable Bioreactors Using Reversible Immobilization of Enzyme on Monolithic Porous Polymer Support With Attached Gold Nanoparticles*. *111*(1), 50–58. https://doi.org/10.1002/bit.25005

Mahmudul, H. M., Hagos, F. Y., Mamat, R., Adam, A. A., Ishak, W. F. W., & Alenezi, R. (2017). Production, characterization and performance of biodiesel as an alternative fuel in diesel engines – A review. *Renewable and Sustainable Energy Reviews*, *72*, 497–509. https://doi.org/10.1016/j.rser.2017.01.001

Malek, M. N. F. A., Pushparaja, L., Hussin, N. M., Embong, N. H., Bhuyar,

P., Rahim, M. H. A., & Maniam, G. P. (2021). Exploration of efficiency of nano calcium oxide (CaO) as catalyst for enhancement of biodiesel production. *Journal of Microbiology, Biotechnology and Food Sciences*, *11*(1), 1–4. https://doi.org/10.15414/jmbfs.3935

Mba, O. I., Dumont, M. J., & Ngadi, M. (2015). Palm oil: Processing, characterization and utilization in the food industry - A review. *Food Bioscience*, *10*, 26–41. https://doi.org/10.1016/j.fbio.2015.01.003

A. Mena-cervantes, V. Y., Gonz, M. A., Guti, A. N., Sosa-rodríguez, F. S., Vazquez-arenas, J., Rodríguez-ramírez, R., & Hern, R. (2022). Green and fast biodiesel production at room temperature using soybean and Jatropha curcas L . oils catalyzed by potassium ferrate. *Journal of Cleaner Production*, 372, 133739. https://doi.org/10.1016/j.jclepro.2022.133739

Mohadesi, M., Gouran, A., & Dehghan Dehnavi, A. (2021). Biodiesel production using low cost material as high effective catalyst in a microreactor. *Energy*, *219*, 119671. https://doi.org/10.1016/j.energy.2020.119671

Muanruksa, P., Wongsirichot, P., Winterburn, J., & Kaewkannetra, P. (2021). Integrated cleaner biocatalytic process for biodiesel production from crude palm oil comparing to refined palm oil. *Catalysts*, *11*(6). https://doi.org/10.3390/catal11060734

Parandi, E., Mousavi, M., Kiani, H., Rashidi Nodeh, H., Cho, J., & Rezania, S. (2023). Optimization of microreactor-intensified transesterification reaction of sesame cake oil (sesame waste) for biodiesel production using magnetically immobilized lipase nano-biocatalyst. *Energy Conversion and Management*, *295*(June), 117616. https://doi.org/10.1016/j.enconman.2023.117616

Ponnumsamy, V. K., Al-Hazmi, H. E., Shobana, S., Dharmaraja, J., Jadhav, D. A., J, R. B., Piechota, G., Igliński, B., Kumar, V., Bhatnagar, A., Chae, K. J., & Kumar, G. (2024). A review on homogeneous and heterogeneous catalytic microalgal lipid extraction and transesterification for biofuel production. *Chinese Journal of Catalysis*, *59*, 97–117. https://doi.org/10.1016/S1872-2067(23)64626-1

Prats, H., Alonso, G., Sayós, R., & Gamallo, P. (2020). Transition metal atoms encapsulated within microporous Silicalite-1 zeolite: A systematic computational study. *Microporous and Mesoporous Materials*, *308*(July). https://doi.org/10.1016/j.micromeso.2020.110462

Riaz, I., Shafiq, I., Jamil, F., Al-Muhtaseb, A. H., Akhter, P., Shafique, S., Park, Y.-K., & Hussain, M. (2024). A review on catalysts of biodiesel (methyl esters) production. *Catalysis Reviews*, *66*(4), 1084–1136. https://doi.org/10.1080/01614940.2022.2108197

Roschat, W., Siritanon, T., Yoosuk, B., & Promarak, V. (2016). Biodiesel production from palm oil using hydrated lime-derived CaO as a low-cost basic heterogeneous catalyst. *Energy Conversion and Management*, *108*, 459–467. https://doi.org/10.1016/j.enconman.2015.11.036

Sabarudin, A., Shu, S., Yamamoto, K., & Umemura, T. (2021). Preparation of metal-immobilized methacrylate-based monolithic columns for flow-through cross-coupling reactions. *Molecules*, *26*(23), 1–14. https://doi.org/10.3390/molecules26237346

Salaheldeen, M., Mariod, A. A., Aroua, M. K., Rahman, S. M. A., Soudagar, M. E. M., & Fattah, I. M. R. (2021). Current state and perspectives on transesterification of triglycerides for biodiesel production. *Catalysts*, *11*(9), 1–37. https://doi.org/10.3390/catal11091121

Satriadi, H., Pratiwi, I. Y., Khuriyah, M., Widayat, Hadiyanto, & Prameswari, J. (2022). Geothermal solid waste derived Ni/Zeolite catalyst for waste cooking oil processing. *Chemosphere*, *286*(Pt 1), 131618. https://doi.org/10.1016/j.chemosphere.2021.131618

Tasfiyati, A. N., Iftitah, E. D., Sakti, S. P., & Sabarudin, A. (2016). Evaluation of glycidyl methacrylate-based monolith functionalized with weak anion exchange moiety inside 0.5 mm i.d. column for liquid chromatographic separation of DNA. *Analytical Chemistry Research*, *7*, 9–16. https://doi.org/10.1016/j.ancr.2015.11.001

Urban, J., Svec, F., & Fréchet, J. M. J. (2012). A monolithic lipase reactor for biodiesel production by transesterification of triacylglycerides into fatty acid methyl esters. *Biotechnology and Bioengineering*, *109*(2), 371–380. https://doi.org/10.1002/bit.23326

Vasić, K. (2020). Biodiesel Production Using Solid Acid Catalysts. *Catalysts*, *10*(237), 1–20. https://doi.org/10.3390/catal10020237

Wan Osman, W. N. A., Rosli, M. H., Mazli, W. N. A., & Samsuri, S. (2024). Comparative review of biodiesel production and purification. *Carbon Capture Science and Technology*, *13*(July), 100264. https://doi.org/10.1016/j.ccst.2024.100264

Widayat, W, Satriadi, H., Setyojati, P.W., Shihab, D., Buchori, L., Hadiyanto, H., Nurushofa, F.A. (2024). Preparation CaO/MgO/Fe3O4 magnetite catalyst and catalytic test for biodiesel production, *Results. Eng. 22.* 102202, https://doi.org/10.1016/j.rineng.2024.102202.

Xie, W., & Huang, M. (2020). Fabrication of immobilized Candida rugosa lipase on magnetic Fe3O4-poly(glycidyl methacrylate-co-methacrylic acid) composite as an efficient and recyclable biocatalyst for enzymatic production of biodiesel. *Renewable Energy*, *158*, 474–486. https://doi.org/10.1016/j.renene.2020.05.172

Yusuf, B. O., Oladepo, S. A., & Ganiyu, S. A. (2024). Efficient and Sustainable Biodiesel Production via Transesterification: Catalysts and Operating Conditions. *Catalysts*, *14*(9), 581. https://doi.org/10.3390/catal14090581

Zhang, Q., Duan, X., Tang, S., Wang, C., Wang, W., & Feng, W. (2023). Catalytic performance of amino acid / phosphotungstic acid as bi-functional heterogeneous catalyst for biodiesel production. *The Environmental Engineering Research(EER)*, *28*(1), 1–8. https://www.eeer.org/new/journal/view.php?number=1376

Zhao, S. Y., Chen, Z. Y., Wei, N., Liu, L., & Han, Z. B. (2019). Highly Efficient Cooperative Catalysis of Single-Site Lewis Acid and Brønsted Acid in a Metal-Organic Framework for the Biginelli Reaction [Rapid-communication]. *Inorganic Chemistry*, *58*(12), 7657–7661. https://doi.org/10.1021/acs.inorgchem.9b00816